The effects of environment on *Arctica islandica* shell formation and architecture

Stefania Milano[1*], Gernot Nehrke[2], Alan D. Wanamaker Jr.[3], Irene Ballesta-Artero[4,5], Thomas Brey[2], Bernd R. Schöne[1]

[1] Institute of Geosciences, University of Mainz, Joh.-J.-Becherweg 21, 55128 Mainz, Germany

[2] Alfred Wegener Institute for Polar and Marine Research, Am Handelshafen 12, 27570 Bremerhaven, Germany

[3] Department of Geological and Atmospheric Sciences, Iowa State University, Ames, Iowa, 50011-3212, USA

[4] Royal Netherlands Institute for Sea Research and Utrecht University, PO Box 59, 1790 AB Den Burg, Texel, The Netherlands

[5] Department of Animal Ecology, VU University Amsterdam, The Netherlands

* Corresponding author. Email: smilano@uni-mainz.de

Keywords: Confocal Raman microscopy; Scanning electron microscopy; Shell microstructure; Water temperature; Diet; Bivalve shell

Abstract

Mollusks record valuable information in their hard parts that reflect ambient environmental conditions. For this reason, shells can serve as excellent archives to reconstruct past climate and environmental variability. However, animal physiology and biomineralization, which are often poorly understood, can make the decoding of environmental signals a challenging task. Many of the routinely used shell-based proxies are sensitive to multiple different environmental and physiological variables. Therefore, the identification and interpretation of individual environmental signals (e.g. water temperature) often is particularly difficult. Additional proxies not influenced by multiple environmental variables or animal physiology would be a great asset in the field of paleoclimatology. The aim of this study is to investigate the potential use of structural properties of *Arctica islandica* shells as an environmental proxy. A total of eleven specimens were analyzed to study if changes of the microstructural organization of this marine bivalve are related to environmental conditions. In order to limit the interference of multiple parameters, the samples were cultured under controlled conditions. Three specimens presented here were grown at two different water temperatures (10 °C and 15 °C) for multiple weeks and exposed only to ambient food conditions. An additional eight specimens were reared under three different dietary regimes. Shell material was analyzed with two techniques: (1) Confocal Raman microscopy (CRM) was used to quantify changes of the orientation of microstructural units and pigment distribution and (2) Scanning electron microscopy (SEM) was used to detect changes in microstructural organization. Our results indicate that *A. islandica* microstructure is not sensitive to changes in the food source, and likely, shell pigment are not altered by diet. However, seawater temperature had a statistically significant effect on the orientation of the biomineral. Although additional work is

required, the results presented here suggest that the crystallographic orientation of biomineral units of *A. islandica* may serve as an alternative and independent proxy for seawater temperature.

1. Introduction

Biomineralization is a process through which living organisms produce a protective, mineralized hard tissue. The considerable diversity of biomineralizing species contributes to high variability in terms of shape, organization and mineralogy of the structures produced (Lowenstam and Weiner, 1989; Carter et al., 2012). Different architectures at the micrometer and nanometer scale and different biochemical compositions determine material properties that serve specific functions (Weiner and Addadi, 1997; Currey, 1999; Merkel et al., 2007). Besides these differences, all mineralized tissues are hybrid materials consisting in hierarchical arrangements of biomineral units surrounded by organic matrix, also known as "microstructures" (Bøggild, 1930; Carter and Clark, 1985; Rodriguez-Navarro et al., 2006) or "ultrastructures" (Blackwell et al., 1977; Olson et al., 2012) or overall "fabrics" (Schöne, 2013; Schöne et al., 2013). The carbonate and organic phases represent the fundamental level of the organization of biomaterials (Aizenberg et al., 2005; Meyers et al., 2006). The mechanisms of microstructure formation and shaping, especially in mollusks, has attracted increasing attention during recent decades. At present, it is commonly accepted that the organic compounds play an important role in the formation of the inorganic phases of biominerals (Weiner and Addadi, 1991; Berman et al., 1993; Dauphin et al., 2003; Nudelman et al., 2006). However, the identification of the exact mechanisms driving biomineralization is still an open research question. Previous studies conducted on mollusks show that environmental parameters

69 can influence microstructure formation (Lutz, 1984; Tan Tiu and Prezant, 1987; Tan Tiu, 1988;
70 Nishida et al., 2012). These results set the stage for a research interest toward the use of shell
71 microstructures as proxies for reconstructing environmental conditions (Tan Tiu, 1988; Tan Tiu
72 and Prezant, 1989; Olson et al., 2012; Milano et al., 2015).

73 Mollusks are routinely used as climate and environmental proxy archives because they can
74 record a large amount of environmental information in their shells (Richardson, 2001; Wanamaker
75 et al., 2011a; Schöne and Gillikin, 2013). Whereas structures at nanometric level are still
76 underexplored as potential environmental recorders, shell patterns at lower magnification, such as
77 individual growth increments, are commonly used for this purpose (Jones, 1983; Schöne et al.,
78 2005; Marali and Schöne, 2015; Mette et al., 2016). Mollusks deposit skeletal material on a
79 periodic basis and at different rates (Thompson et al., 1980; Deith, 1985). During periods of fast
80 growth, growth increments are formed whereas during periods of slower growth, growth lines are
81 formed (Schöne, 2008; Schöne and Gillikin, 2013). The periodicity of such structures ranges from
82 tidal to annual (Gordon and Carriker, 1978; Schöne and Surge, 2012). By crossdating time-series
83 with similar growth patterns it is possible to construct century and millennia-long master
84 chronologies (Marchitto et al., 2000; Black et al. 2008; Black et al., 2016; Butler et al., 2013). This
85 basic approach, in combination with geochemical methods, has great potential in reconstructing
86 past climatic conditions (Wanamaker et al., 2011b). At present, the most frequently used and well-
87 accepted geochemical proxy is oxygen isotopic composition of shell material ($\delta^{18}O_{shell}$) (Epstein,
88 1953; Grossman and Ku, 1986; Schöne et al., 2004; Wanamaker et al., 2007) which may serve as
89 a paleothermometer and/or paleosalinometer (Mook, 1971; Andrus, 2011); however, $\delta^{18}O_{shell}$ value
90 is influenced by both seawater temperature and the isotopic composition of seawater ($\delta^{18}O_{water}$;
91 related to salinity). Thus, $\delta^{18}O_{shell}$-based temperature reconstructions are particularly challenging
92 in habitats with fluctuating $\delta^{18}O_{water}$ conditions such as estuaries or restricted basins (Gillikin et al.,

2005). Because of the multiple impacts on $\delta^{18}O_{shell}$ values, there have been substantial efforts to develop alternative techniques to reconstruct environmental variables from mollusk shells (Schöne et al., 2010; Milano et al., 2017).

This study investigates the possibility using shell microstructure properties to serve as a new environmental proxy. For this purpose, the effects of seawater temperature (grown at 10 °C and 15 °C) and dietary regime on the microstructural units of *Arctica islandica* cultured under controlled conditions were analyzed and quantified. *A. islandica* was chosen as model species because of its great potential in paleoclimatology and paleoceanography (see Schöne, 2013; Wanamaker et al., 2016). Its extreme longevity of up to more than 500 years makes this species a highly suitable archive for long-term paleoclimate and environmental reconstructions (Schöne et al., 2005; Wanamaker et al., 2008; Wanamaker et al., 2012; Butler et al., 2013).

2. Materials and Methods

The analyses were conducted on eleven *A. islandica* shells. Three juvenile *A. islandica* shells, sampled for the seawater temperature experiment, were collected alive on November 21, 2009 aboard the *F.V. Three of a Kind* off Jonesport, Maine USA (44° 26′ 9.829″N, 67° 26′ 18.045″W) in 82 m water depth. From 2009 to 2011, all animals were kept in a flowing seawater laboratory at the Darling Marine Center, Walpole, Maine, USA (see Beirne et al., 2012 for additional details). In 2011, clams were grown at two different temperature regimes for 16 weeks (Table 1). At the completion of the experiment, shells were estimated to be between 4 to 5 years old. Eight one-year

115 old juveniles were collected in July 2014 from Kiel Bay, Baltic Sea (54° 32′ N, 10° 42′ E; Fig. 1)
116 and kept alive in tanks at 7 °C for six months at the Alfred Wegener Institute for Polar and Marine
117 Research (AWI), Bremerhaven, Germany. During this time interval, the animals were fed with an
118 algal mix of *Nannochloropsis* sp., *Isochrysis galbana* and *Pavlova lutheri.* Then, they were
119 transferred to the Royal Netherlands Institute for Sea Research (NIOZ), Texel, The Netherlands,
120 and cultured in tanks at three different dietary conditions for 11 weeks (Table 1).

121

122

123 ## 2.1 Seawater temperature experiment

124 The seawater temperature experiment started on 27 March 2011 and ended on 21 July 2011. Prior
125 to the start of the experiment the animals were marked with calcein. The staining leaves a clear
126 fluorescent marker in the shells that can be used to identify which shell material has formed prior
127 to and during the experiment. Initially, the animals were kept at 10.3 ± 0.2 °C for 48 days. Then,
128 they were briefly removed from the tanks and marked again. Subsequently, the clams were cultured
129 for 69 more days at 15.0 ± 0.3 °C. Ambient seawater was pumped from the adjacent Damariscotta
130 River estuary and adjusted to desired temperature. The salinity was measured with a Hydrolab®
131 MiniSonde. It ranged between 30.2 ± 0.7 and 30.7 ± 0.7, in the two experimental phases,
132 respectively. During the entire culture period, all clams were exposed to ambient food conditions.
133 At the end of the experiment the soft tissues were removed.

134

135

136 ## 2.2 Food experiment

137 The food experiment was carried out from 9 February 2015 to 29 April 2015. The animals were
138 placed in aquaria inside a climate room at 9 °C. Water temperature in the tanks ranged between 8
139 and 10 °C. Water salinity was measured by using an ENDECO 102 refractometer and ranged
140 between 29.6 and 29.9 ± 0.1 in each aquarium. The 15-liter tanks were constantly supplied with
141 aerated water from the Wadden Sea. The clams were acclimated for three weeks before the start of
142 the experiment. Three dietary regimes were chosen. One treatment consisted of feeding the animals
143 with Microalgae Mix (food type 1), a ready-made solution of four marine microalgae (25 %
144 *Isochrysis,* 25 % *Tetraselmis,* 25 % *Thalassiosira,* 25 % *Nannochloropsis*) with a particle size
145 range of 2 - 30 µm. A second treatment was based on PhytoMaxx (food type 2), a solution of living
146 *Nannochloropsis* algae with 2 - 5 µm size range. A third treatment served as control, i.e., the
147 animals were not fed with any additional food. In treatments with food type 1 and 2, microalgae
148 were provided at the constant optimum concentration of 20×10^6 cells/liter (Winter, 1969). A
149 dispenser equipped with a timer was used to distribute the food five times per day. At the end of
150 the experiment the soft tissues were removed. A distinct dark line in the shells indicated the
151 transposition to the NIOZ aquaria and the associated stress. This line marks the beginning of the
152 tank experiment.

153

154

155 ## 2.3 Sample preparation

156 The right valve of each specimen was cut into two 1.5 millimeter-thick sections along the axis of
157 maximum growth. For this purpose, a low speed precision saw (Buehler Isomet 1000) was used.
158 Given the small size and fragility of the juvenile shells used in the food experiment, the valves
159 were fully embedded in a block of Struers EpoFix (epoxy) and air-dried overnight prior the

sectioning. Sections of the clams used in the temperature experiment were embedded in epoxy after the cutting. All samples were ground using a Buehler Metaserv 2000 machine equipped with Buehler silicon carbide papers of different grit sizes (P320, P600, P1200, P2500). In addition, the samples were manually ground with Buehler P4000 grit paper and polished with a Buehler diamond polycrystalline suspension (3 μm). Sample surfaces were rinsed in demineralized water and air-dried. In the samples of the temperature experiment, the calcein marks were located under a fluorescence light microscope (Zeiss Axio Imager.A1m microscope equipped with a Zeiss HBO100 mercury lamp and filter set 38: excitation wavelength, ca. 450 - 500 nm; emission wavelength, ca. 500 - 550 nm).

2.4 *A. islandica* shell organization

The shell of *A. islandica* consists of pure aragonite and it is divided in two major layers, an outer (OSL) and the inner shell layer (ISL). The OSL is further subdivided in outer (oOSL) and inner portion (iOSL) (Schöne, 2013). These layers are characterized by specific microstructures (Ropes et al., 1984; Fig. 2). The oOSL largely consists of homogenous microstructure with granular aspect (Schöne et al., 2013). This type of architecture is characterized by approximately equidimensional units of about 5 μm in width. The unit shape tends to be irregular with a bulky aspect. The organization lacks of specific structural arrangement typical of other type of microstructures such as the crossed-lamellar and cross-acicular microstructures. The latter are the main component characterizing the iOSL and ISL (Dunca et al., 2009). Here, elongated units are arranged with two main dip directions, resulting in a relative oblique alignment. As shown in Fig. 2, the elongation of the structures becomes more evident in the ISL.

183 The present study focuses on ventral margin of the shells. Analyses were carried out exclusively in
184 the OSL.

185 Similar to other mollusks, the shell of *A. islandica* contains pigment polyenes which are
186 obviously visible when using CRM (Hedegaard et al., 2006). Polyenes are organic compounds
187 containing single (C-C) and double (C=C) carbon-carbon bonds forming a polyenic chain. Their
188 distribution across the shell is not homogenous. The pigments are abundant in the oOSL whereas
189 they become scarce in the iOSL. Furthermore, an enrichment in polyenes has been observed in the
190 growth lines, potentially indicating their involvement in the biomineralization process (Stemmer
191 and Nehrke, 2014). However, the specific functions of these organic compounds have not been
192 disclosed yet (Hedegaard et al., 2006; Karampelas et al., 2009). Given the high phenotypic
193 variation in pigmentation among and within mollusk species, it has been proposed that coloration
194 does not have a primary function as adaptive tool (i.e. camouflage, warning signaling) as in other
195 animals (Seilacher, 1972; Evans et al., 2009). This, in turn, can indicate a certain degree of
196 influence of the environment on the pigments, in particular by diet (Hedegaard et al., 2006;
197 Soldatov et al., 2013). In the current study, the effect of different dietary regimes was tested in
198 order to explore the potential of polyenes as environmental proxy.

199

200

201 ## 2.5 Confocal Raman microscopy and image processing

202 Shells were mapped with a WITec alpha 300 R (WITec GmbH, Germany) confocal Raman
203 microscope. Scans of 50 × 50 µm, 100 × 50 µm and 150 × 50 µm were performed using a
204 piezoelectric scanner table. All Raman measurements were carried out using a 488 nm diode laser.

A spectrometer (UHTS 300, WITec, Germany) was used with a 600 mm^{-1} grating, a 500 nm blaze and an integration time of 0.03 s. On each sample two to six scans were made, depending of the thickness of the shell. For instance, in juvenile shells (food experiment), two scans of each sample were made. On larger shells used in the temperature experiment, six maps were completed, i.e., two maps in the oOSL, two in the middle of the iOSL and two in the inner portion of the iOSL. Each scan contained between 40,000 and 120,000 data points, depending on the map size. The spatial resolution equaled 250 nm. Half of the maps were performed on the shell portion formed before the experiments. The other half were made on the shell portion formed under experimental conditions. In order to avoid areas affected by transplantation or marking stress, the scans were located far off the calcein and stress lines. Raman maps on food experiment shells were performed 300 µm away from the stress line. In the shells from the temperature experiment, the scans were made 1 mm away from the calcein mark.

Polarized Raman microscopy is known to provide comprehensive information about the crystallographic properties of the materials (Hopkins and Farrow, 1985). The aragonite spectrum is characterized by two lattice modes (translation mode T_a, 152cm^{-1} and librational mode L_a, 206cm^{-1}) and the two internal modes (in-plane band ν_4, 705cm^{-1} and symmetric stretch ν_1, 1085cm^{-1}). The ratio ($R_{v1/Ta}$) between peak intensities belonging to ν_1 and T_a is caused by different crystallographic orientations of the aragonitic units (Hopkins and Farrow, 1985; Nehrke and Nouet, 2011). Within each scan, $R_{v1/Ta}$ was calculated for each data point. New spectral images were generated using WITecProject software (version 4.1, WITec GmbH, Germany). These images were then binarized by replacing all values above 2.5 with 1 and the others with 0. The orientation was quantified by calculating the area formed by pixels of value 1 over the total scan area. The imaging software Gwyddion (http://gwyddion.net/last checked: June 2016) was used for this purpose. The results were expressed in percentage.

The Raman scans of the food experiment shells were analyzed to investigate the pigment composition. Polyene peaks have definite positions in the spectrum according to the number of the C-C and C=C bonds of the chain, which are specific for certain types of pigments. The two major polyene peaks at ~ 1130 (R_1) and 1520 cm^{-1} (R_4) were identified by using the "multipeak fitting 2" routine of IGOR Pro (version 7.00, WaveMetrics, USA). Their exact position was determined adopting a Gaussian fitting function (Fig. 3). The number of single (N_1) and double carbon bonds (N_4) was calculated by applying the equations by Schaffer et al. (1991):

(1) $N_1 = 476 (R_1 - 1{,}082)$

(2) $N_4 = 830 (R_4 - 1{,}438)$

Spectral images of the R_4 band were used to locate the polyenes in the shell and measure the thickness of the pigmented layer. The images were analyzed using the software Panopea (© Schöne and Peinl). The thickness of the pigmented layer was calculated as distance between the outer shell margin and the point where the concentration of polyenes suddenly declined. The measurements were taken perpendicular to the shell outer margin. This analysis was conducted only on the shells of the food experiment. Given the larger size of the shells used in the temperature experiment, the spectral maps were not sufficient for a correct localization of the pigmented layer boundaries and estimation of its thickness.

To quantify changes of the orientation of individual biomineral units of the juvenile shells (food experiment), the spectral maps were subdivided into two portions. The outermost shell portion (oOSL) was enriched in pigments whereas the iOSL showed a decrease in polyene content.

2.6 Scanning electron microscopy

After performing Raman measurements, the samples were prepared for SEM analysis. Each shell slab was ground with a Buehler Metaserv 2000 machine and Buehler silicon F2500 grit carbide paper. To reduce the impact of grinding on the sample surface of juvenile shells, extra grinding was done by hand. Then, the slabs were polished with a Buehler diamond polycrystalline suspension (3 μm). Afterward, shell surfaces were etched in 0.12 N HCl solution for 10 (food experiment samples) to 90 s (temperature experiment samples) and subsequently placed in 6 vol % NaClO solution for 30 min. After being rinsed in demineralized water, air-dried samples were sputter-coated with a 2 nm-thick platinum film by using a Low Vacuum Coater Leica EM ACE200.

A scanning electron microscope (LOT Quantum Design 2nd generation Phenom Pro desktop SEM) with backscattered electron detector and 10 kV accelerating voltage was used to analyze the shells. Images were taken at the same distances from the calcein and stress lines as in the case of the Raman measurements to assure comparability of the data.

In addition, stitched SEM images of the ventral margins were used to accurately determine the shell growth advance during the culturing experiments. Growth increment widths were measured with the software Panopea. Given the difference in duration of the two phases of the temperature experiment, the measurements were expressed as total growth and instantaneous growth rate (Fig. 4a + b). The latter was calculated using the following equation (Brey et al., 1990; Witbaard et al., 1997):

$$\text{Instantaneous growth rate} = (\ln (y_t / y_0) / a) \quad (3)$$

where y_0 represents the initial shell height, y_t is the final shell height and a is the duration of the experiment. In the case of the food experiment, only the total growth was calculated (Fig. 4c).

3. Results

3.1 Effect of seawater temperature and diet on *A. islandica* shell growth

When exposed to a water temperature of 10 °C, the shells grew between 11.67 and 14.17 mm during a period of 48 days. During a period of 69 days at 15 °C, the growth ranged between 2.32 and 5.77 mm (Fig. 4a). Instantaneous growth rate showed a decrease between the two experimental phases. At 10 and 15 °C, the average instantaneous growth per day was 0.0091 and 0.0013, respectively (Fig. 4b). The decrease in total growth and growth rate between the two temperatures was statistically significant (*t*-test, $p < 0.01$).

During the food experiment, shells grew between 0.37 and 3.71 mm with large differences due to the different food types. Growth of specimens exposed to food type 1 ranged between 1.87 to 3.71 mm, whereas those cultured with food type 2 grew between 0.55 to 0.96 mm. Both control specimens added 0.37 mm of shell during the experimental phase (Fig. 4c). ANOVA and Tukey´s HSD post hoc tests showed significant differences between specimens cultured with food type 1 and 2 ($p < 0.05$) and between food type 1 and control shells ($p < 0.05$).

3.2 Effect of seawater temperature on *A. islandica* microstructure

293 At a water temperature of 10 °C, the area occupied by microstructural units oriented with $R_{v1/Ta}$
294 higher than 2.5 a.u. (= arbitrary units) ranged between 31.3 and 50.6 % in the oOSL and between
295 21.3 and 33.5 % in the iOSL. When exposed to 15 °C, values ranged between 25.6 and 48.7 % and
296 between 45.7 and 55.9 % in the oOSL and iOSL, respectively (Fig. 5). Whereas the slight difference
297 of area with $R_{v1/Ta} > 2.5$ in the oOSL was not significant between the two water temperatures (*t*-
298 test, $p = 0.62$), the area with $R_{v1/Ta} > 2.5$ in the iOSL significantly increased at 15 °C (*t*-test, $p =$
299 0.02). Under the SEM, no difference was visible between units formed at 10 °C and 15 °C (Fig. 6).

300

301

302 ## 3.3 Effect of food on *A. islandica* microstructure and pigments

303 In the shells cultured with food type 1, the area occupied by biomineral units oriented with $R_{v1/Ta}$
304 higher than 2.5 a.u. during the experiment ranged between 24.8 % (oOSL) and 43.0 % (iOSL). In
305 the shell portion deposited during the acclimation phase, the ratio varied between 19.4 % (oOSL)
306 and 36.2 % (iOSL). Although a trend was recognized, these variations were not statistically
307 different (*t*-tests. OSL: $p = 0.43$; ISL: $p = 0.57$; Fig. 7a). On the contrary, in the clams exposed to
308 food type 2, the area occupied by units oriented with $R_{v1/Ta} > 2.5$ ranged between 11.7 % (oOSL)
309 and 20.4 % (iOSL). Before the experiment, the proportions were higher, i.e., 18.1% (oOSL) and
310 26.3% (iOSL) (Fig. 7b). As for the other treatment, the difference was not significant (*t*-tests.
311 oOSL: $p = 0.34$; iOSL: $p = 0.28$). In the control shells grown with no extra food supply, the area
312 with $R_{v1/Ta} > 2.5$ ranged between 24.6 % (oOSL) and 44.8 % (iOSL) during the experiment and
313 21.2 % (oOSL) and 44.5 % (iOSL) before the experiment (Fig. 7c). Hence, no trend was visible
314 and the two portions did not show significant differences (*t*-tests. oOSL: $p = 0.59$; iOSL: $p = 0.99$).

315 As for the temperature experiment, under the SEM, the microstructure of the shells from the food
316 experiment did not show any change (Fig. 9).

317 All treatments showed a slightly thicker pigmented layer formed during the experiment than
318 during the acclimation phase (Fig. 9a). During the experiment, clams cultured with food type 1
319 showed, on average, a thickening by 6.4 %. In the food type 2 specimens, the layer thickness
320 increased by 9.9 %. Control shells showed an increase of 10.4 % (Fig. 9b). However, none of these
321 differences was statistically significant (*t*-test. Food type 1: $p = 0.43$; Food type 2: $p = 0.39$; Control:
322 $p = 0.10$). According to the position of the polyene peaks, the number of single carbon bonds in the
323 pigment chain did not change between the acclimation and experimental phase ($N_1 = 10.1 \pm 1.3$
324 and $N_1 = 10.0 \pm 0.9$, respectively). Likely, no significant variation was observed in the number of
325 double carbon bonds ($N_4 = 10.5 \pm 0.2$ and $N_4 = 10.4 \pm 0.3$, respectively; Table 2).

326

327

328

329

330 # 4. Discussion

331 According to the results, variations of both food type and water temperature can influence the shell
332 production rate of *A. islandica.* However, the shell microstructure and pigmentation react
333 differently to these two environmental variables. Whereas changes of the dietary conditions do not
334 affect the shell architecture and pigment composition, the crystallographic orientation of the
335 biomineral units responds to seawater temperature fluctuations.

4.1 Environmental influence on shell microstructure

The environmental conditions experienced by mollusks during the process of biomineralization appear to influence shell organization (Carter, 1980). Among the different environmental variables, water temperature is the most studied driving force of structural changes of the shell. For instance, shell mineralogy can vary depending on water temperature (Carter, 1980). According to the thermal potentiation hypothesis, nucleation and growth of calcitic structural units is favored at low temperatures by kinetic factors (Carter et al., 1998). As a consequence, bivalve species living in cold water environments exhibit additional or thicker calcitic layers compared to the corresponding species from warm waters (Lowenstam, 1954; Taylor and Kennedy, 1969). Changes in the calcium carbonate polymorph also affect the type of microstructures (Milano et al., 2016). However, architectural variations often occur without mineralogical impact (Carter, 1980).

The present results indicate that temperature induces a change in the crystallographic orientation of the biomineral units of *A. islandica*. Although water temperature was previously shown to have an impact on microstructure formation, the attention has been mainly addressed to the effects on the morphometric characteristics (e.g. size and shape) or on the type of microstructure. Milano et al. (2017) demonstrated that size and elongation of prismatic structural units of *Cerastoderma edule* were positively correlated to seawater temperature variation throughout the growing season. Likely, low temperatures induced the formation of small nacre tablets in *Geukensia demissa* (Lutz, 1984). Seasonal changes of the microstructural type were reported in the freshwater bivalve *Corbicula fluminea* (Prezant and Tan Tiu, 1986; Tan Tiu and Prezant, 1989). During the warm months, crossed acicular structure was produced, whereas simple

crossed-lamellae were formed during the winter period. So far, variations of the crystallographic properties of bivalve biominerals have been exclusively investigated as a response to hypercapnic (acidified) conditions. *Mytilus galloprovincialis* and *Mytilus edulis* showed a significant change in the orientation of the prisms forming shell calcitic layer when subjected to hypercapnia (Hahn et al., 2012; Fitzer et al., 2014). Altered crystallographic organization may derive from the animal exposure to suboptimal conditions. These findings together with the present results suggest that thermal- and hypercapnic-induced stress are likely to affect the ability of the bivalves to preserve the orientation of their microstructural units (Fitzer et al., 2015).

Different food sources do not significantly influence the orientation of the biomineral units or the composition and distribution of pigments in shells of *A. islandica*. In previous studies, the relationship between microstructure and diet was virtually overlooked resulting in a lack of data in the literature. As suggested by Hedegaard et al. (2006), however, the type of polyenes is influenced by food. The ingestion of pigment-enriched microalgae potentially leads to an accumulation of pigments in mollusk tissues and the shell (Soldatov et al., 2013). On the other hand, it has been argued that polyenes do not generate from food sources like other pigments (i.e., carotenoids), but they are locally synthesized (Karampelas et al., 2009). In accordance to Stemmer and Nehrke (2014), the results presented here support the view that the specific diets on which the animals rely on do not influence shell pigment composition. The chemical characteristics of the polyenes are likely to be species-specific and independent from the habitats.

4.2 Confocal Raman microscopy as tool for microstructural analysis

From a methodological perspective, the present study represents an innovative approach in the investigation of shell microstructural organization. Electron backscatter diffraction (EBSD) has been previously used to determine the crystallographic orientation of gastropod (Fryda et al., 2009; Pérez-Huerta et al., 2011) and bivalve microstructural units (Checa et al., 2006; Frenzel et al., 2012; Karney et al., 2012). Whereas, CRM on mollusk shells is generally applied within studies on taphonomic mineralogical alteration and pigment identification (Stemmer and Nehrke, 2014; Beierlein et al., 2015). Both techniques provide considerably high spatially resolved analysis up to 250 nm, allowing the identification of individual structural units at µm- and nm-scale (Cusack et al., 2008; Karney et al., 2012). CRM offers important advantages supporting a broader application of this methodology in the biomineralization research field. For instance, samples do not require any pre-treatment. Unlike EBSD, there is no need of preparing thin-sections (~ 150 µm thick) or etching the shell surface (Griesshaber et al., 2010; Hahn et al., 2012). Therefore, further structural and geochemical analyses can be easily performed on the same sections (Nehrke et al., 2012). In addition, the size of CRM scans can be remarkably large (~ 7-8 mm^2) without compromising the achievable resolution. By overlapping adjacent scans, it is possible to produce stitched scans allowing to further increase the region of interest on the shell surface. On the other side, EBSD provides a relevant advantage to take into consideration. It allows absolute measures of the crystallographic orientation of the carbonate structures. The CRM, instead, determines the relative change in the orientation between the single units without providing absolute values.

SEM has previously been demonstrated to provide a convenient approach for the identification of individual structural units and the quantification of potential changes occurring within them (Milano et al., 2017, 2016b). However, SEM exclusively provides information about the morphometric characteristics of the microstructural units. As highlighted by the present study, to achieve an exhaustive examination, it is suggested to combine SEM with techniques assessing

crystallographic properties of the biomaterials. For instance, our results show that the effect of water temperature is detectable in crystallographic orientation but not in morphometric features of the biomineral units.

4.3 Environmental influence on shell growth

Numerous previous studies demonstrated that growth rate of *A. islandica* is linked to environmental variables (e.g., Witbaard et al., 1997, 1999; Schöne et al., 2004; Butler et al., 2010; Mette et al., 2016). However, the relative importance of the main factors, temperature and food supply/quality driving shell formation are still not well understood. Positive correlations between shell growth and water temperature have been identified (i.e., Schöne et al., 2005; Wanamaker et al., 2009; Marali et al., 2015), but the relationship between shell growth and environment is more complex (Marchitto et al., 2010; Stott et al., 2010; Schöne et al., 2013) and likely dependent on the synergic effect of food availability and water temperature (Butler et al., 2013; Lohmann and Schöne, 2013; Mette et al., 2016). Tank experiments were run in order to precisely identify the role of these two parameters of shell growth of *A. islandica* (Witbaard et al., 1997; Hiebenthal et al., 2012). A tenfold increase in instantaneous growth rate was observed between 1 and 12 °C, with the greatest variation occurring below 6 °C (Witbaard et al., 1997). On the contrary, a temperature increase between 4 and 16 °C was shown to produce a slowdown of shell production (Hiebenthal et al., 2012). Our results are in agreement with the latter study and show a decrease in the instantaneous growth rate between 10 and 15 °C. High temperatures are often associated with an increase of free radical production (Abele et al., 2002). A large amount of energy then has to be allocated to limit oxidative cellular damage (Abele and Puntarulo, 2004). This translates into a higher accumulation of lipofuscin and slower shell production rate (Hiebenthal et al., 2013). The contrasting results of

428 previous studies may be explained by individual differences in the tolerance toward temperature
429 change (Marchitto et al., 2000).

430 Along with water temperature, food availability was also shown to influence *A. islandica*
431 shell growth (Witbaard et al., 1997). At high algal cell densities, the siphon activity increased. This,
432 in turn, was positively correlated to shell growth. Previous experiments used different combinations
433 of algae such as *Isochrysis galbana* and *Dunaliella marina* (Witbaard et al., 1997), or
434 *Nannochloropsis oculata, Phaeodactylum tricornutum* and *Chlorella* sp. (Hiebenthal et al., 2012)
435 to grow the clams. However, there are still uncertainties about the composition of the primary food
436 source for this species (Butler et al., 2010). Even though it is challenging to determine the preferred
437 algal species, our results show that the use of a mixture of different algal species results in
438 significantly faster shell growth than the used of just one algal species. In the natural environment,
439 suspension feeders such as *A. islandica* preferentially ingest certain particle sizes (Rubenstein and
440 Koehl, 1977; Jorgensen, 1996; Baker et al., 1998). The exposure to a limited algal size range, as in
441 the case of food type 2, may affect shell growth. Furthermore, multispecific solutions contain a
442 higher variability of biochemical components that better meet the nutritional requirements of the
443 animal (Widdows, 1991). Our results are in good agreement with previous findings. For instance,
444 it has been shown by Strömgren and Cary (1984) that *Mytilus edulis* shell growth increased as a
445 result of a diet based on three different algal species. Furthermore, Epifanio (1979) tested the
446 differences on the growth of *Crasssostrea virginica* and *Mercenaria mercenaria* of a mixed diet
447 composed by *Isochrysis galbana* and *Thalassiosira pseudonana* and diets consisting of the single
448 species. Faster growth was measured in the mixed diet treatment, indicating a synergic effect of
449 the relative food composition (Epifanio, 1979). Likely, *Mytilus edulis* grew faster when reared with
450 different types of mixed diets as opposed to monospecific diets (Galley et al., 2010).

5. Conclusions

Arctica islandica shell growth and biomineral orientation vary with changes in seawater temperature. However, exposure to different food sources affect shell deposition rate but do not influence the organization of the biomineral units. Given the exclusive sensitivity to one environmental variable, the orientation of biomineral units may represent a promising new temperature proxy for paleoenvironmental reconstructions. However, additional studies are needed to further explore the subject. In particular, intra-individual variability influence on the results needs to be assessed. In the present study, a variation in the orientation between individuals was well visible and the risks associated have to be taken in account when considering further application of the possible proxy. Furthermore, the effect of other environmental variables such as salinity needs to be tested.

The innovative application of CRM for microstructural orientation and proxy development proved that the technique has large potential in this research direction. More studies are needed to validate its suitability in paleoclimatology experimental works.

Acknowledgements

The authors acknowledge the crew of the *F.V. Three of a Kind* for helping with the collection of the animals. Design and execution of the seawater temperature experiment were successfully realized thanks to the support of B. Beal, D. Gillikin, A. Lorrain and the Darling Marine Center scientific team. Funding for this study was kindly provided by the EU within the framework of the Marie Curie International Training Network ARAMACC (604802).

References

Abele, D., Heise, K., Pörtner, H. O. and Puntarulo, S.: Temperature-dependence of mitochondrial function and production of reactive oxygen species in the intertidal mud clam *Mya arenaria*, J. Exp. Biol., 205, 1831-1841, doi:10.1016/j.ecolind.2011.04.007, 2002.

Abele, D. and Puntarulo, S.: Formation of reactive species and induction of antioxidant defence systems in polar and temperate marine invertebrates and fish, Comp. Biochem. Physiol. Part A, 138(4), 405-415, doi:10.1016/j.cbpb.2004.05.013, 2004.

Aizenberg, J., Weaver, J. C., Thanawala, M. S., Sundar, V. C., Morse, D. E. and Fratzl, P.: Skeleton of Euplectella sp.: structural hierarchy from the nanoscale to the macroscale, Science, 309(5732), 275-278, doi:10.1126/science.1112255, 2005.

Andrus, C. F. T.: Shell midden sclerochronology, Quat. Sci. Rev., 30(21-22), 2892-2905, doi:10.1016/j.quascirev.2011.07.016, 2011.

Baker, S. M., Levinton, J. S., Kurdziel, J. P. and Shumway, S. E.: Selective feeding and biodeposition by zebra mussels and their relation to changes in phytoplankton composition and seston load, J. Shellfish Res., 17, 1207-1213, 1998.

Beierlein, L., Nehkre, G. and Brey, T.: Confocal Raman microscopy in sclerochronology: A powerful tool to visualize environmental information in recent and fossil biogenic archives, Geochemistry Geophys. Geosystems, 16, 325-335, doi:10.1002/2014GC005684.Key, 2015.

Beirne, E. C., Wanamaker, A. D. and Feindel, S. C.: Experimental validation of environmental controls on the $\delta^{13}C$ of *Arctica islandica* (ocean quahog) shell carbonate, Geochim. Cosmochim. Acta, 84, 395-409, doi:10.1016/j.gca.2012.01.021, 2012.

Berman, A., Hanson, J., Leiserowitz, L., Koetzle, T. F., Weiner, S. and Addadi, L.: Biological control of crystal texture: a widespread strategy for adapting crystal properties to function, Science, 259(5096), 776-779, doi:10.1126/science.259.5096.776, 1993.

Black, B. A., Gillespie, D. C., MacLellan, S. E. and Hand, C. M.: Establishing highly accurate production-age data using the tree-ring technique of crossdating: a case study for Pacific geoduck (*Panopea abrupta*), Can. J. Fish. Aquat. Sci., 65, 2572-2578, doi:10.1139/F08-158, 2008.

Black, B. A., Griffin, D., van der Sleen, P., Wanamaker, A. D., Speer, J. H., Frank, D. C., Stahle, D. W., Pederson, N., Copenheaver, C. A., Trouet, V., Griffin, S. and Gillanders, B. M.: The value of crossdating to retain high-frequency variability, climate signals, and extreme events in environmental proxies, Glob. Chang. Biol., 22(7), 2582-2595, doi:10.1111/gcb.13256, 2016.

512 Bøggild, O. B.: The shell structure of the mollusks, in Det Kongelige Danske Videnskabernes
513 Selskabs Skrifter, Natruvidenskabelig og Mathematisk, pp. 231-326, Afdeling., 1930.

514 Brey, T., Arntz, W. E., Pauly, D. and Rumohr, H.: *Arctica (Cyprina) islandica* in Kiel Bay (Western
515 Baltic): growth, production and ecological significance, J. Exp. Mar. Bio. Ecol., 136(3), 217-
516 235, doi:10.1016/0022-0981(90)90162-6, 1990.

517 Butler, P. G., Richardson, C. A., Scourse, J. D., Wanamaker, A. D. Jr, Shammon, T. M. and
518 Bennell, J. D.: Marine climate in the Irish Sea: analysis of a 489-year marine master
519 chronology derived from growth increments in the shell of the clam *Arctica islandica*, Quat.
520 Sci. Rev., 29(13-14), 1614-1632, doi:10.1016/j.quascirev.2009.07.010, 2010.

521 Butler, P. G., Wanamaker, A. D. Jr, Scourse, J. D., Richardson, C. A. and Reynolds, D. J.:
522 Variability of marine climate on the North Icelandic Shelf in a 1357-year proxy archive based
523 on growth increments in the bivalve *Arctica islandica*, Palaeogeogr. Palaeoclimatol.
524 Palaeoecol., 373, 141-151, doi:10.1016/j.palaeo.2012.01.016, 2013.

525 Carter, J. G.: Environmental and biological controls of bivalve shell mineralogy and
526 microstructure, in Skeletal Growth of Aquatic Organisms: Biological Records of
527 Environmental Change (Topics in Geobiology), edited by D. C. Rhoads and R. A. Lutz, pp.
528 69-113, Plenum, N. Y, 1980.

529 Carter, J. G. and Clark, G. R. I.: Classification and phylogenetic significance of molluscan shell
530 microstructure, in Mollusks, Notes for a Short Course, edited by T. W. Broadhead, pp. 50-
531 71., 1985.

532 Carter, J. G., Barrera, E. and Tevesz, M. T. S.: Thermal potentiation and mineralogical evolution
533 in the Bivalvia (Mollusca), J. Paleontol., 72(6), 991-1010, 1998.

534 Carter, J. G., Harries, P. J., Malchus, N., Sartori, A. F., Anderson, L. C., Bieler, R., Bogan, A. E.,
535 Coan, E. V., Cope, J. C. W., Cragg, S. M., Garcia-March, J. R., Hylleberg, J., Kelley, P.,
536 Kleemann, K., Kriz, J., McRoberts, C., Mikkelsen, P. M., Pojeta, J. J., Temkin, I., Yancey,
537 T. and Zieritz, A.: Illustrated glossary of the bivalvia, Treatise Online, 1(48), 2012.

538 Checa, A. G., Okamoto, T. and Ramírez, J.: Organization pattern of nacre in Pteriidae (Bivalvia:
539 Mollusca) explained by crystal competition., Proc. Biol. Sci., 273(1592), 1329-37,
540 doi:10.1098/rspb.2005.3460, 2006.

541 Currey, J. D.: The design of mineralised hard tissues for their mechanical functions, J. Exp. Biol.,
542 202, 3285-3294, 1999.

543 Cusack, M., Parkinson, D., Freer, A., Pérez-Huerta, A., Fallick, A. E. and Curry, G. B.: Oxygen
544 isotope composition in *Modiolus modiolus* aragonite in the context of biological and
545 crystallographic control, Mineral. Mag., 72(2), 569-577,
546 doi:10.1180/minmag.2008.072.2.569, 2008.

547 Dauphin, Y., Cuif, J. P., Doucet, J., Salomé, M., Susini, J. and Willams, C. T.: In situ chemical
548 speciation of sulfur in calcitic biominerals and the simple prism concept, J. Struct. Biol.,
549 142(2), 272-280, doi:10.1016/S1047-8477(03)00054-6, 2003.

550 Deith, M. R.: The composition of tidally deposited growth lines in the shell of the edible cockle,
551 *Cerastoderma edule*, J. Mar. Biol. Assoc. United Kingdom, 65(3), 573-581, 1985.

552 Dunca, E., Mutvei, H., Göransson, P., Mörth, C.-M., Schöne, B. R., Whitehouse, M. J., Elfman,
553 M. and Baden, S. P.: Using ocean quahog (*Arctica islandica*) shells to reconstruct
554 palaeoenvironment in Öresund, Kattegat and Skagerrak, Sweden, Int. J. Earth Sci., 98(1), 3-
555 17, doi:10.1007/s00531-008-0348-6, 2009.

556 Epifanio, C. E.: Growth in bivalve molluscs: nutritional effects of two or more species of algae in
557 diets fed to the American oyster *Crassostrea virginica* (Gmelin) and the hard clam
558 *Mercenaria mercenaria* (L.), Aquaculture, 18, 1-12, 1979.

559 Epstein, S., Buchbaum, R., Lowenstam, H. A. and Urey, H. C.: Revised carbonate-water isotopic
560 temperature scale. Bull. Geol. Soc. Am., 64, 1315-1326, 1953.

561 Evans, S., Camara, M. D. and Langdon, C. J.: Heritability of shell pigmentation in the Pacific
562 oyster, *Crassostrea gigas*, Aquaculture, 286 (3-4), 211-216,
563 doi:10.1016/j.aquaculture.2008.09.022, 2009.

564 Fitzer, S. C., Cusack, M., Phoenix, V. R. and Kamenos, N. A.: Ocean acidification reduces the
565 crystallographic control in juvenile mussel shells, J. Struct. Biol., 188, 39-45,
566 doi:10.1016/j.jsb.2014.08.007, 2014.

567 Fitzer, S. C., Zhu, W., Tanner, K. E., Phoenix, V. R., Nicholas, A. K. and Cusack, M.: Ocean
568 acidification alters the material properties of *Mytilus edulis* shells, J. R. Soc. Interface,
569 12(103), doi:10.1098/rsif.2014.1227Published, 2015.

570 Frenzel, M., Harrison, R. J. and Harper, E. M.: Nanostructure and crystallography of aberrant
571 columnar vaterite in *Corbicula fluminea* (Mollusca), J. Struct. Biol., 178(1), 8-18,
572 doi:10.1016/j.jsb.2012.02.005, 2012.

573 Fryda, J., Bandel, K. and Frydova, B.: Crystallographic texture of Late Triassic gastropod nacre:
574 Evidence of long-term stability of the mechanism controlling its formation, Bull. Geosci.,
575 84(4), 745-754, doi:10.3140/bull.geosci.1169, 2009.

576 Galley, T. H., Batista, F. M., Braithwaite, R., King, J. and Beaumont, A. R.: Optimisation of larval
577 culture of the mussel *Mytilus edulis* (L.), Aquac. Int., 18(3), 315-325, doi:10.1007/s10499-
578 009-9245-7, 2010.

579 Gillikin, D. P., De Ridder, F., Ulens, H., Elskens, M., Keppens, E., Baeyens, W. and Dehairs, F.:
580 Assessing the reproducibility and reliability of estuarine bivalve shells (*Saxidomus*
581 *giganteus*) for sea surface temperature reconstruction: Implications for paleoclimate studies,
582 Palaeogeogr. Palaeoclimatol. Palaeoecol., 228(1-2), 70-85,
583 doi:10.1016/j.palaeo.2005.03.047, 2005.

584 Gordon, J. and Carriker, M. R.: Growth lines in a bivalve mollusk: subdaily patterns and dissolution
585 of the shell, Science, 202, 519-521, doi:10.1126/science.202.4367.519, 1978.

586 Griesshaber, E., Neuser, R. D. and Schmahl, W. W.: The application of EBSD analysis to
587 biomaterials : microstructural and crystallographic texture variations in marine carbonate
588 shells, Semin Soc Esp Miner., 7, 22-34, 2010.

589 Grossman, E. L. and Ku, T.: Oxygen and carbon isotope fractionation in biogenic aragonite:
590 Temperature effects, Chem. Geol., 59, 59-74, 1986.

591 Hahn, S., Rodolfo-Metalpa, R., Griesshaber, E., Schmahl, W. W., Buhl, D., Hall-Spencer, J. M.,
592 Baggini, C., Fehr, K. T. and Immenhauser, A.: Marine bivalve shell geochemistry and
593 ultrastructure from modern low pH environments: environmental effect versus experimental
594 bias, Biogeosciences, 9, 1897-1914, doi:10.5194/bg-9-1897-2012, 2012.

595 Hedegaard, C., Bardeau, J. F. and Chateigner, D.: Molluscan shell pigments: An in situ resonance
596 Raman study, J. Molluscan Stud., 72(2), 157-162, doi:10.1093/mollus/eyi062, 2006.

597 Hiebenthal, C., Philipp, E., Eisenhauer, A. and Wahl, M.: Interactive effects of temperature and
598 salinity on shell formation and general condition in Baltic Sea *Mytilus edulis* and *Arctica*
599 *islandica*, Aquat. Biol., 14(3), 289-298, doi:10.3354/ab00405, 2012.

600 Hiebenthal, C., Philipp, E. E. R., Eisenhauer, A. and Wahl, M.: Effects of seawater pCO_2 and
601 temperature on shell growth, shell stability, condition and cellular stress of Western Baltic
602 Sea *Mytilus edulis* (L.) and *Arctica islandica* (L.), Mar. Biol., 160, 2073-2087,
603 doi:10.1007/s00227-012-2080-9, 2013.

604 Hopkins, J. B. and Farrow, L. A.: Raman microprobe determination of local crystal orientation, J.
605 Appl. Phys., 59(4), 1103-1110, doi:10.1063/1.336547, 1985.

606 Jones, D. S.: Sclerochronology: Shell record of the molluscan shell, Am. Sci., 71(4), 384-391,
607 1983.

608 Jorgensen, C. B.: Bivalve filter feeding revisited, Mar. Ecol. Prog. Ser., 142(1-3), 287-302,
609 doi:10.3354/meps142287, 1996.

610 Karampelas, S., Fritsch, E., Mevellec, J. Y., Sklavounos, S. and Soldatos, T.: Role of polyenes in
611 the coloration of cultured freshwater pearls, Eur. J. Mineral., 21(1), 85-97, doi:10.1127/0935-
612 1221/2009/0021-1897, 2009.

613 Karney, G. B., Butler, P. G., Speller, S., Scourse, J. D., Richardson, C. A., Schröder, M., Hughes,
614 G. M., Czernuszka, J. T. and Grovenor, C. R. M.: Characterizing the microstructure of
615 *Arctica islandica* shells using NanoSIMS and EBSD, Geochemistry, Geophys. Geosystems,
616 13(4), doi:10.1029/2011GC003961, 2012.

Lohmann, G. and Schöne, B. R.: Climate signatures on decadal to interdecadal time scales as obtained from mollusk shells (*Arctica islandica*) from Iceland, Palaeogeogr. Palaeoclimatol. Palaeoecol., 373, 152-162, doi:10.1016/j.palaeo.2012.08.006, 2013.

Lowenstam, H. A.: Factors affecting the aragonite: calcite ratios in carbonate-secreting marine organisms, J. Geol., 62(3), 284-322, 1954.

Lowenstam, H. A. and Weiner, S.: On biomineralization, Oxford University Press, New York., 1989, pp.324.

Lutz, R. A.: Paleoecological implications of environmentally-controlled variation in molluscan shell microstructure, Geobios, 17, 93-99, doi:10.1016/S0016-6995(84)80161-8, 1984.

Marali, S. and Schöne, B. R.: Oceanographic control on shell growth of *Arctica islandica* (Bivalvia) in surface waters of Northeast Iceland - Implications for paleoclimate reconstructions, Palaeogeogr. Palaeoclimatol. Palaeoecol., 420, 138-149, doi:10.1016/j.palaeo.2014.12.016, 2015.

Marchitto, T. M., Jones, G. A., Goodfriend, G. A. and Weidman, C. R.: Precise temporal correlation of Holocene mollusk shells using sclerochronology, Quat. Res., 53, 236-246, doi:10.1006/qres.1999.2107, 2000.

Merkel, C., Griesshaber, E., Kelm, K., Neuser, R., Jordan, G., Logan, A., Mader, W. and Schmahl, W. W.: Micromechanical properties and structural characterization of modern inarticulated brachiopod shells, J. Geophys. Res., 112(G02008), doi:10.1029/2006JG000253, 2007.

Mette, M. J., Wanamaker, A. D., Carroll, M. L., Ambrose, W. G. and Retelle, M. J.: Linking large-scale climate variability with *Arctica islandica* shell growth and geochemistry in northern Norway, Limnol. Oceanogr., 61(2), 748-764, doi:10.1002/lno.10252, 2016.

639 Milano, S., Prendergast, A. L. and Schöne, B. R.: Effects of cooking on mollusk shell structure and
640 chemistry: Implications for archeology and paleoenvironmental reconstruction, J. Archaeol.
641 Sci. Reports, 7, 14-26, doi: 10.1016/j.jasrep.2016.03.045, 2016.

642 Milano, S., Schöne, B. R., Wang, S. and Müller, W. E.: Impact of high pCO_2 on shell structure of
643 the bivalve *Cerastoderma edule*, Mar. Environ. Res., 119, 144-155,
644 doi:10.1016/j.marenvres.2016.06.002, 2016b.

645 Milano, S., Schöne, B. R. and Witbaard, R.: Changes of shell microstructural characteristics of
646 *Cerastoderma edule* (Bivalvia) - A novel proxy for water temperature, Palaeogeogr.
647 Palaeoclimatol. Palaeoecol., doi:10.1016/j.palaeo.2015.09.051, 2017.

648 Mook, W.: Paleotemperatures and chlorinities from stable carbon and oxygen isotopes in shell
649 carbonate, Palaeogeogr. Palaeoclimatol. Palaeoecol., 9(4), 245-263, doi:10.1016/0031-
650 0182(71)90002-2, 1971.

651 Nehrke, G. and Nouet, J.: Confocal Raman microscope mapping as a tool to describe different
652 mineral and organic phases at high spatial resolution within marine biogenic carbonates: case
653 study on *Nerita undata* (Gastropoda, Neritopsina), Biogeosciences, 8, 3761-3769,
654 doi:10.5194/bg-8-3761-2011, 2011.

655 Nishida, K., Ishimura, T., Suzuki, A. and Sasaki, T.: Seasonal changes in the shell microstructure
656 of the bloody clam, *Scapharca broughtonii* (Mollusca: Bivalvia: Arcidae), Palaeogeogr.
657 Palaeoclimatol. Palaeoecol., 363-364, 99-108, doi:10.1016/j.palaeo.2012.08.017, 2012.

658 Nudelman, F., Gotliv, B. A., Addadi, L. and Weiner, S.: Mollusk shell formation: mapping the
659 distribution of organic matrix components underlying a single aragonitic tablet in nacre, J.
660 Struct. Biol., 153, 176-187, doi:10.1016/j.jsb.2005.09.009, 2006.

661 Pérez-Huerta, A., Dauphin, Y., Cuif, J. P. and Cusack, M.: High resolution electron backscatter
662 diffraction (EBSD) data from calcite biominerals in recent gastropod shells, Micron, 42(3),
663 246-51, doi:10.1016/j.micron.2010.11.003, 2011.

664 Pérez-Huerta, A., Etayo-Cadavid, M. F., Andrus, C. F. T., Jeffries, T. E., Watkins, C., Street, S. C.
665 and Sandweiss, D. H.: El Niño impact on mollusk biomineralization-implications for trace
666 element proxy reconstructions and the paleo-archeological record. PLoS One, 8(2), e54274,
667 doi:10.1371/journal.pone.0054274, 2013.

668 Prezant, R. S. and Tan Tiu, A.: Spiral crossed-lamellar shell growth in *Corbicula* (Mollusca:
669 Bivalvia), Trans. Am. Microsc. Soc., 105(4), 338-347, 1986.

670 Richardson, C. A.: Molluscs as archives of environmental change, Oceanogr. Mar. Biol. an Annu.
671 Rev., 39, 103-164, 2001.

672 Rodríguez-Navarro, A. B., CabraldeMelo, C., Batista, N., Morimoto, N., Alvarez-Lloret, P.,
673 Ortega-Huertas, M., Fuenzalida, V. M., Arias, J. I., Wiff, J. P. and Arias, J. L.: Microstructure
674 and crystallographic-texture of giant barnacle (*Austromegabalanus psittacus*) shell, J. Struct.
675 Biol., 156, 355-362, doi:10.1016/j.jsb.2006.04.009, 2006.

676 Ropes, J. W., Jones, D. S., Murawski, S. A., Serchuk, F. M. and Jearld, A.: Documentation of
677 annual growth lines in ocean quahogs, *Artica islandica* Linne, Fish. Bull., 82(1), 1-19, 1984.

678 Rubenstein, D. I. and Koehl, M. A. R.: The mechanisms of filter feeding: some theoretical
679 considerations, Am. Nat., 111, 981-994, 1977.

680 Schaffer, H. E., Chance, R. R., Silbey, R. J., Knoll, K. and Schrock, R. R.: Conjugation length
681 dependence of Raman scattering in a series of linear polyenes: Implications for
682 polyacetylene, J. Chem. Phys., 94(6), 4161, doi:10.1063/1.460649, 1991.

683 Schöne, B. R.: The curse of physiology—challenges and opportunities in the interpretation of
684 geochemical data from mollusk shells, Geo-Marine Lett., 28, 269-285, doi:10.1007/s00367-
685 008-0114-6, 2008.

686 Schöne, B. R.: *Arctica islandica* (Bivalvia): a unique paleoenvironmental archive of the northern
687 North Atlantic Ocean, Glob. Planet. Change, 111, 199-225,
688 doi:10.1016/j.gloplacha.2013.09.013, 2013.

689 Schöne, B. R. and Gillikin, D. P.: Unraveling environmental histories from skeletal diaries —
690 Advances in sclerochronology, Palaeogeogr. Palaeoclimatol. Palaeoecol., 373, 1-5,
691 doi:10.1016/j.palaeo.2012.11.026, 2013.

692 Schöne, B. R. and Surge, D. M.: Part N , revised , volume 1 , chapter 14 : bivalve sclerochronology
693 and geochemistry, Treatise Online, 1(46), 1-24, 2012.

694 Schöne, B. R., Freyre Castro, A. D., Fiebig, J., Houk, S. D., Oschmann, W. and Kröncke, I.: Sea
695 surface water temperatures over the period 1884-1983 reconstructed from oxygen isotope
696 ratios of a bivalve mollusk shell (*Arctica islandica*, southern North Sea), Palaeogeogr.
697 Palaeoclimatol. Palaeoecol., 212, 215-232, doi:10.1016/j.palaeo.2004.05.024, 2004.

698 Schöne, B. R., Fiebig, J., Pfeiffer, M., Gleß, R., Hickson, J., Johnson, A. L. A., Dreyer, W. and
699 Oschmann, W.: Climate records from a bivalved Methuselah (*Arctica islandica*, Mollusca;
700 Iceland), Palaeogeogr. Palaeoclimatol. Palaeoecol., 228(1-2), 130-148,
701 doi:10.1016/j.palaeo.2005.03.049, 2005.

702 Schöne, B. R., Zhang, Z., Jacob, D., Gillikin, D. P., Tütken, T., Garbe-Schönberg, D.,
703 McConnaughey, T. and Soldati, A.: Effect of organic matrices on the determination of the

trace element chemistry (Mg, Sr, Mg/Ca, Sr/Ca) of aragonitic bivalve shells (*Arctica islandica*) - Comparison of ICP-OES and LA-ICP-MS data, Geochem. J., 44, 23-37, 2010.

Schöne, B. R., Radermacher, P., Zhang, Z. and Jacob, D. E.: Crystal fabrics and element impurities (Sr/Ca, Mg/Ca, and Ba/Ca) in shells of *Arctica islandica*—Implications for paleoclimate reconstructions, Palaeogeogr. Palaeoclimatol. Palaeoecol., 373, 50-59, doi:10.1016/j.palaeo.2011.05.013, 2013.

Seilacher, A.: Divaricate patterns in pelecypod shells, Lethaia, 5(3), 325-343, doi:10.1111/j.1502-3931.1972.tb00862.x, 1972.

Soldatov, A. A., Gostyukhina, O. L., Borodina, A. V. and Golovina, I. V.: Qualitative composition of carotenoids, catalase and superoxide dismutase activities in tissues of bivalve mollusc *Anadara inaequivalvis* (Bruguiere, 1789), J. Evol. Biochem. Physiol., 49(4), 3889-398, doi:10.1134/S0022093013040026, 2013.

Stemmer, K. and Nehrke, G.: The distribution of polyenes in the shell of *Arctica islandica* from North Atlantic localities: a confocal Raman microscopy study, J. Molluscan Stud., 80, 365-370, doi:10.1093/mollus/eyu033, 2014.

Stott, K. J., Austin, W. E. N., Sayer, M. D. J., Weidman, C. R., Cage, A. G. and Wilson, R. J. S.: The potential of *Arctica islandica* growth records to reconstruct coastal climate in north west Scotland, UK, Quat. Sci. Rev., 29(13-14), 1602-1613, doi:10.1016/j.quascirev.2009.06.016, 2010.

Strömgren, T. and Cary, C.: Growth in length of *Mytilus edulis* L. fed on different algal diets, J. Exp. Mar. Bio. Ecol., 76(1), 23-34, doi:10.1016/0022-0981(84)90014-5, 1984.

Tan Tiu, A.: Temporal and spatial variation of shell microstructure of *Polymesoda caroliniana* (Bivalvia: Heterodonta), Am. Malacol. Bull., 6(2), 199-206, 1988.

Tan Tiu, A. and Prezant, R. S.: Temporal variation in microstructure of the inner shell surface of *Corbicula fluminea* (Bivalvia: Heterodonta), Am. Malacol. Bull., 7(1), 65-71, 1989.

Tan Tiu, A. and Prezant, R. S.: Shell microstructural responses of *Geukensia demissa granosissima* (Mollusca: Bivalvia) to continual submergence, Am. Malacol. Bull., 5(2), 173-176, 1987.

Taylor, J.D. and Kennedy, W.J.: The shell structure and mineralogy of *Chama pellucida* inst electron microscope, Veliger 11: 391-398, 1969.

Thompson, I., Jones, D. S. and Dreibelbis, D.: Annual internal growth banding and life history of the ocean quahog *Artica islandica* (Mollusca: Bivalvia), Mar. Biol., 57, 25-34, 1980.

Wanamaker, A. D., Kreutz, K. J., Borns, H. W., Introne, D. S., Feindel, S., Funder, S., Rawson, P. D. and Barber, B. J.: Experimental determination of salinity, temperature, growth, and metabolic effects on shell isotope chemistry of *Mytilus edulis* collected from Maine and Greenland, Paleoceanography, 22(2), doi:10.1029/2006PA001352, 2007.

Wanamaker, A. D., Heinemeier, J., Scourse, J. D., Richardson, C. A., Butler, P. G., Eiríksson, J. and Knudsen, K. L.: Very long-lived mollusks confirm 17th century ad tephra-based radiocarbon reservoir ages for North Icelandic shelf waters, Radiocarbon, 50(3), 399-412, 2008.

Wanamaker, A. D., Kreutz, K. J., Schöne, B. R., Maasch, K. A., Pershing, A. J., Borns, H. W., Introne, D. S. and Feindel, S.: A late Holocene paleo-productivity record in the western Gulf of Maine, USA, inferred from growth histories of the long-lived ocean quahog (*Arctica islandica*), Int. J. Earth Sci., 98(1), 19-29, doi:10.1007/s00531-008-0318-z, 2009.

747 Wanamaker, A. D., Hetzinger, S. and Halfar, J.: Reconstructing mid- to high-latitude marine
748 climate and ocean variability using bivalves, coralline algae, and marine sediment cores from
749 the Northern Hemisphere, Palaeogeogr. Palaeoclimatol. Palaeoecol., 302(1), 1-9,
750 doi:10.1016/j.palaeo.2010.12.024, 2011a.

751 Wanamaker, A. D., Butler, P. G., Scourse, J. D., Heinemeier, J., Eiríksson, J., Knudsen, K. L. and
752 Richardson, C. A.: Surface changes in the North Atlantic meridional overturning circulation
753 during the last millennium, Paleoceanography, 3, 237-252, doi:10.1038/ncomms1901, 2012.

754 Wanamaker, A. D., Mette, M. J. and Whitney, N.: The potential for the long- lived bivalve *Arctica*
755 *islandica* to contribute to our understanding of past AMOC dynamics, US CLIVAR Var., 14,
756 13-19, 2016.

757 Wanamaker, A. D., Kreutz, K. J., Schöne, B. R. and Introne, D. S.: Gulf of Maine shells reveal
758 changes in seawater temperature seasonality during the Medieval Climate Anomaly and the
759 Little Ice Age, Palaeogeogr. Palaeoclimatol. Palaeoecol., 302(1), 43-51,
760 doi:10.1016/j.palaeo.2010.06.005, 2011b.

761 Weiner, S. and Addadi, L.: Acidic macromolecules of mineralized tissues: the controllers of crystal
762 formation, Trends Biochem. Sci., 16, 252-256, 1991.

763 Weiner, S. and Addadi, L.: Design strategies in mineralized biological materials, J. Mater. Chem.,
764 7, 689-702, doi:10.1039/a604512j, 1997.

765 Widdows, J.: Physiological ecology of mussel larvae, Aquaculture, 94(2-3), 147-163,
766 doi:10.1016/0044-8486(91)90115-N, 1991.

767 Winter, J. E.: Über den Einfluß der Nahrungskonzentration und anderer Faktoren auf
768 Filtrierleistung und Nahrungsausnutzung der Muscheln Arctica islandica und Modiolus
769 modiolus, Mar. Biol., 4(2), 87-135, doi:10.1007/BF00347037, 1969.

770 Witbaard, R., Franken, R. and Visser, B.: Growth of juvenile *Arctica islandica* under experimental
771 conditions, Helgolaender Meeresuntersuchungen, 51, 417-431, doi:10.1007/BF02908724,
772 1997.

773 Witbaard, R., Duineveld, G. C. A. and de Wilde, P. A. W. J.: Geographical differences in growth
774 rates of *Arctica islandica* (Mollusc: Bivalvia) from the North Sea and adjacent waters, J. Mar.
775 Biol. Assoc. United Kingdom, 79, 907-915, 1999.

776

777

778 # Figures and tables

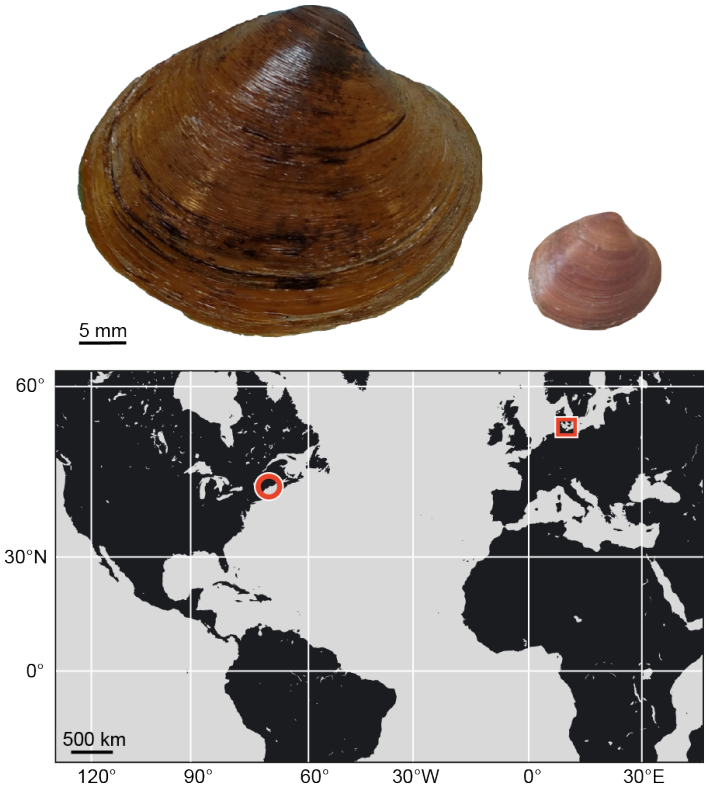

779

780 **Fig. 1.** Shell of adult *Arctica islandica* used in the temperature experiment (left) and juvenile from the Baltic

781 Sea used in the food experiment (right). The map indicates the localities where the two sets of shells were

782 collected: Jonesport, Maine (circle) and Kiel Bay (square).

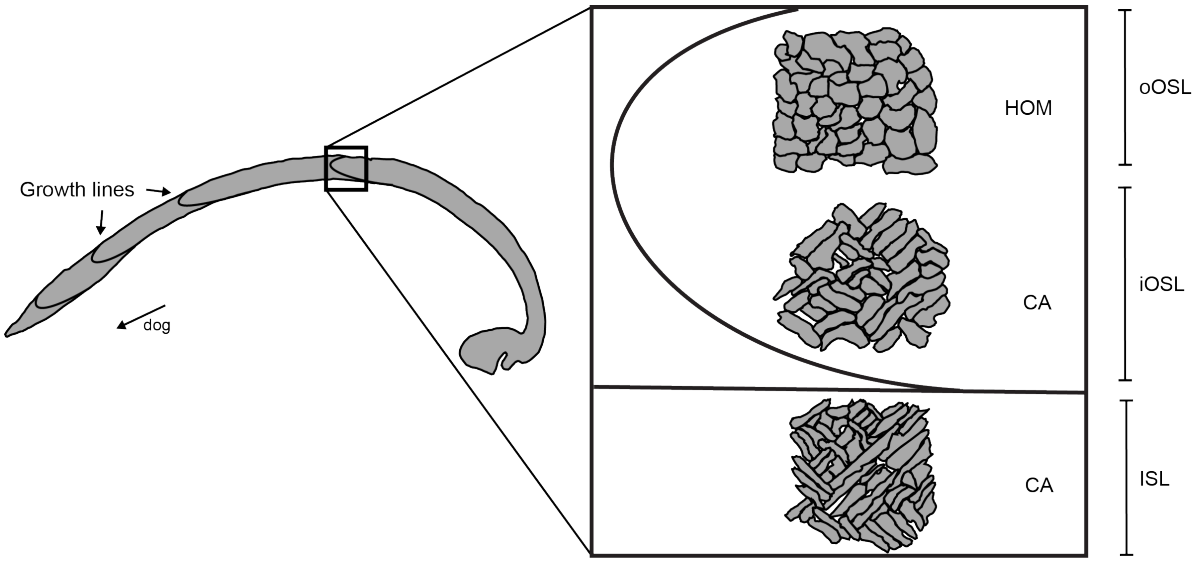

783

784 **Fig. 2.** Sketch showing the microstructures characterizing the different shell layers of *Arctica islandica.* The
785 oOSL is formed by homogenous microstructure (HOM), whereas the oOSL and ISL are composed of
786 crossed acicular structure (CA). dog = direction of growth.

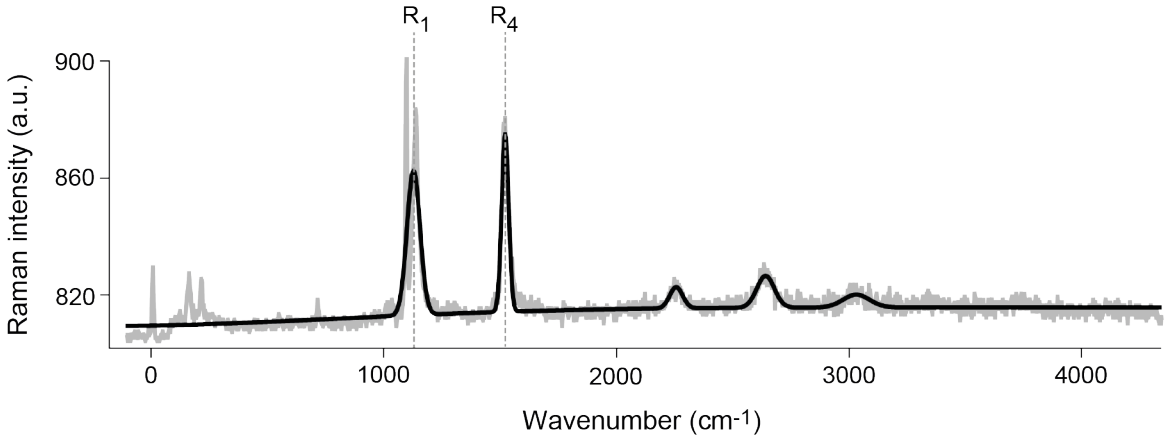

787

788 **Fig. 3.** Raman spectrum of *Arctica islandica* showing the typical aragonite peaks (grey line). The exact
789 position of the polyene peaks R_1 and R_4 was determined by using a peak fitting routine based on a Gaussian
790 function (black line).

791

792

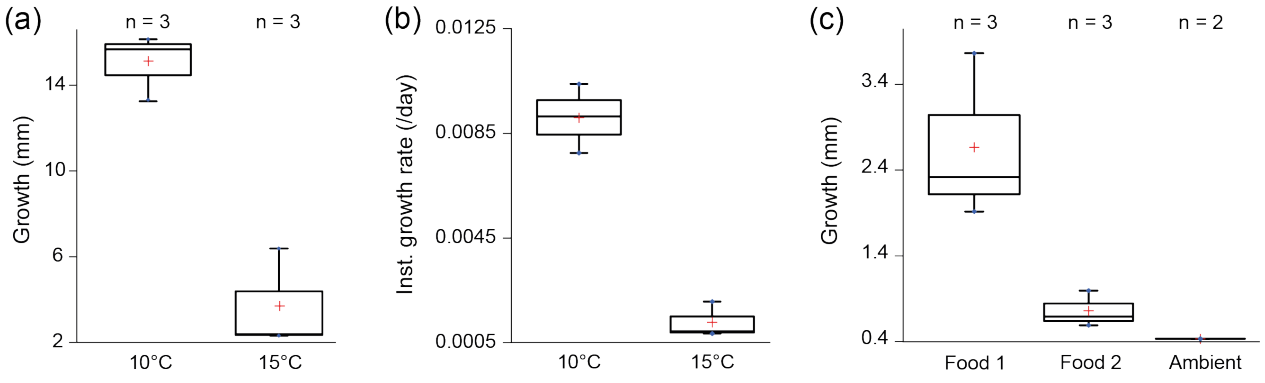

793

794 **Fig. 4.** *Arctica islandica* shell growth under controlled conditions. (a) Total growth and (b) instantaneous
795 growth rate during the temperature experiment. (c) Total growth during the food experiment.

796

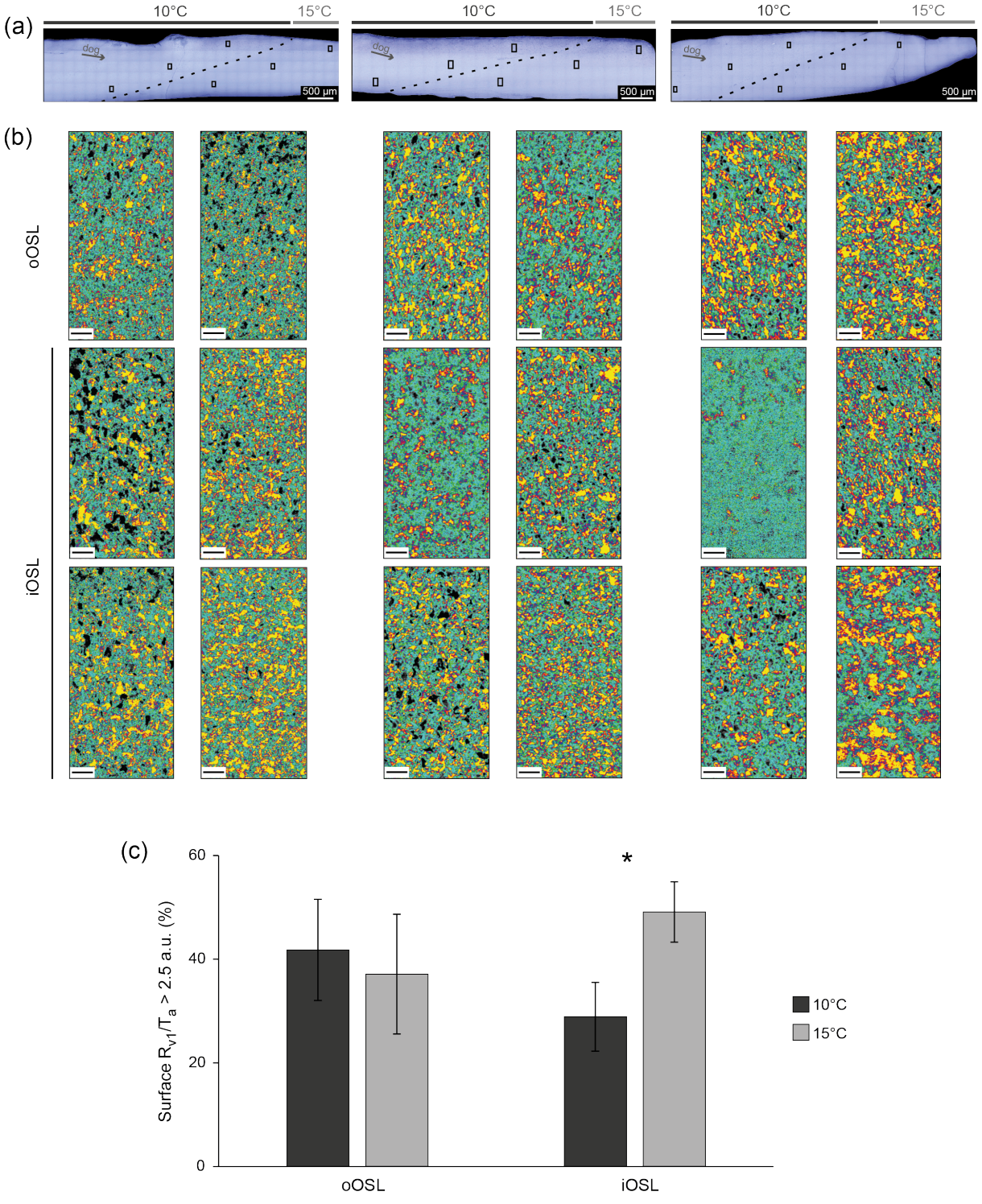
(a)
10°C
15°C
10°C
15°C
10°C
15°C
dog
dog
dog
500 µm
500 µm
500 µm
(b)
oOSL
iOSL
(c)
Surface R_{v1}/T_a > 2.5 a.u. (%)
60
40
20
0
*
10°C
15°C
oOSL
iOSL

Fig. 5. Effect of temperature increase on biomineral orientation. (a) Position of the Raman maps of the three specimens reared at 10 °C and 15 °C. Dotted lines indicate the location of the calcein marks. dog = direction of growth. (b) Raman spectral maps of $R_{v1/Ta}$. Left images of each column represents shell portion formed at 10 °C, right images represent shell portions formed at 15 °C. First row of pairs refers to oOSL, the other two represent the iOSL. Scale bars = 10 µm. (c) Proportions of biominerals with $R_{v1/Ta} > 2.5$ a.u. with respect to the total map area. Asterisks indicate significant difference between the orientation of iOSL microstructures formed at 10 and 15°C ($p < 0.05$).

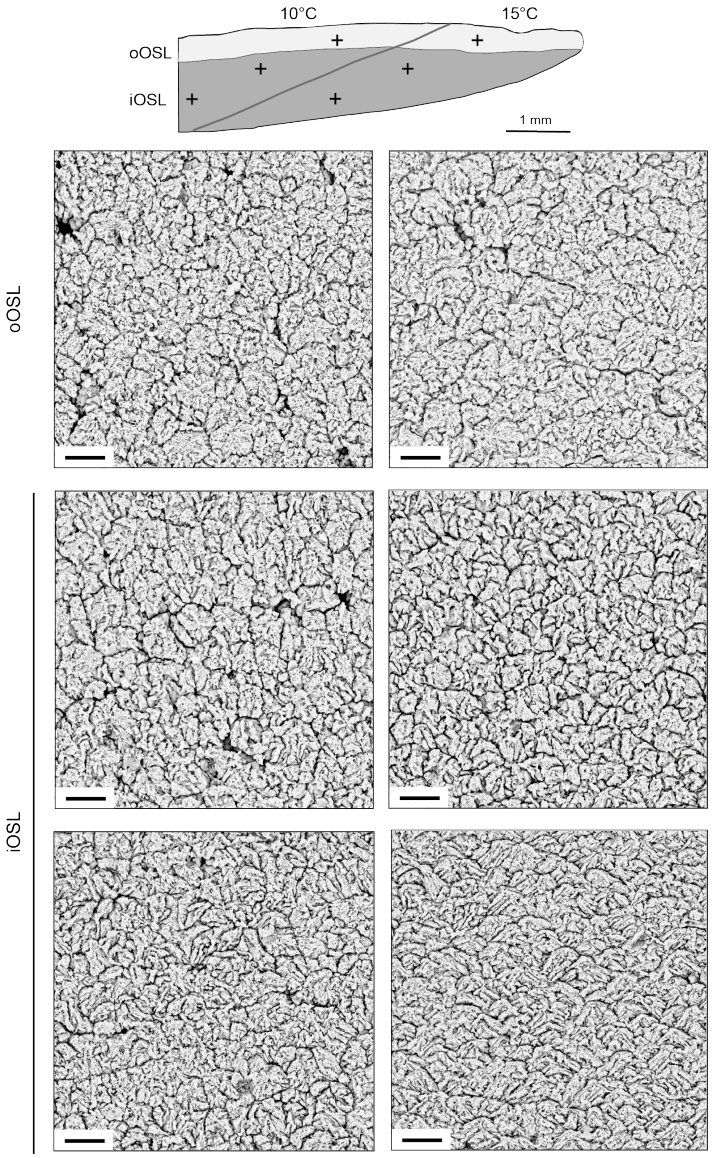

Fig. 6. SEM images of *Arctica islandica* shell microstructures formed at 10 °C (left column) and at 15 °C (right column). The sketch indicates the position of the images 1 mm away from the calcein mark (grey line). The first row of images refers to the oOSL, the other two row refers to the iOSL. Scale bars if not otherwise indicated = 5 µm.

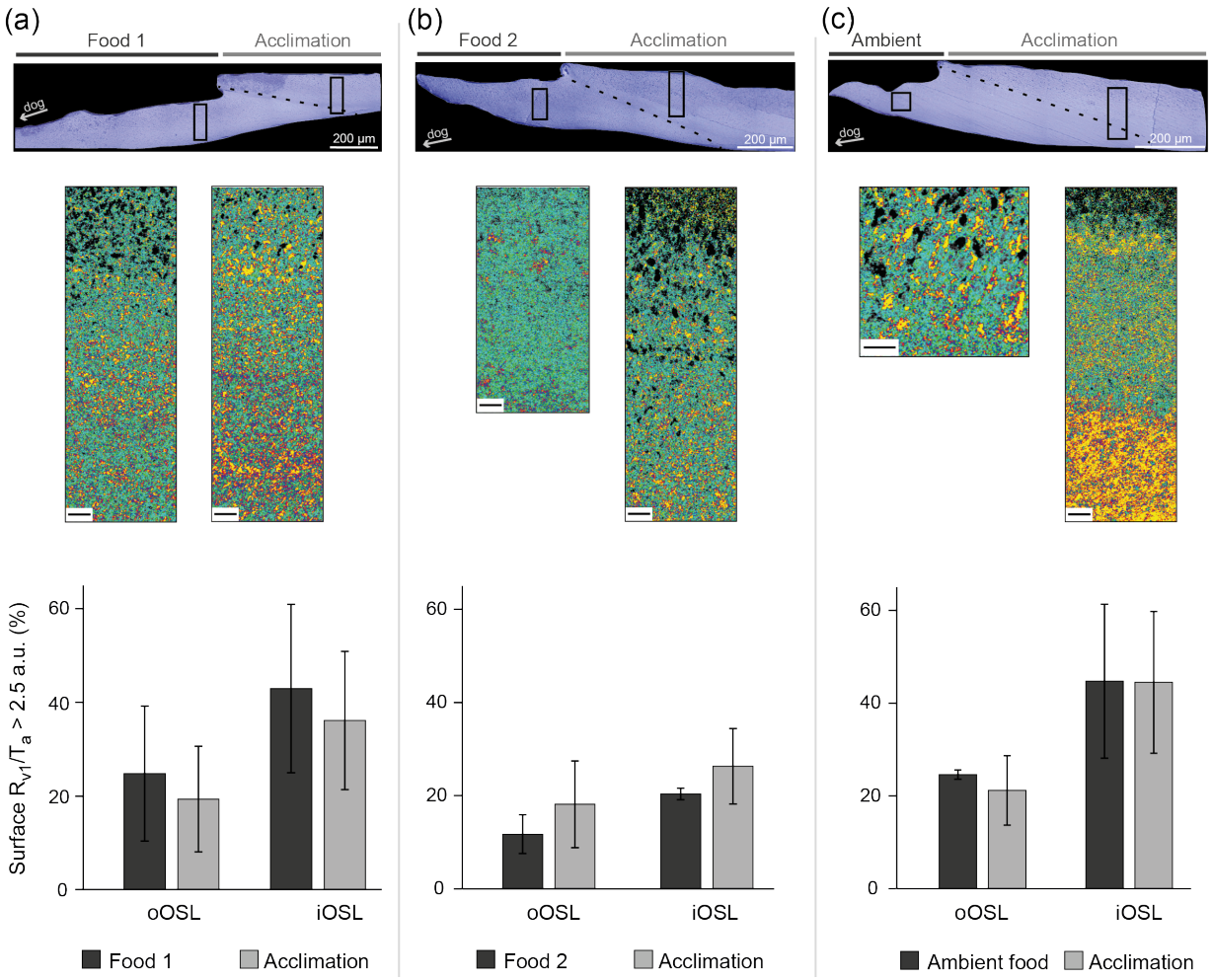

817

818 **Fig. 7.** Effect of different diets based on (a) food type 1, (b) food type 2 and (c) ambient food on biomineral
819 orientation. The optical microscope images indicate the position of the Raman scans. Dotted line marks the
820 start of the experiment. The portion of shell prior the line was formed during the acclimation phase. dog =
821 direction of growth. The Raman spectral maps indicate the ratio $R_{v1/Ta}$ for each data point of the scan. For
822 each shell, maps on the left represent shell portions during the experiment, maps on the right represent shell
823 portions formed during the acclimation phase. In the acclimation portion of the sample reared with ambient
824 food, a significant change in the microstructure orientation is visible. The respective area of the Raman map
825 was not considered in further calculations because it was influenced by the emersion and transportation
826 stress at the start of the experiment. Scale bars = 10 µm. The graphs show the proportions of biominerals of
827 oOSL and iOSL with $R_{v1/Ta}$ > 2.5 a.u. with respect to the total map area.

828

829

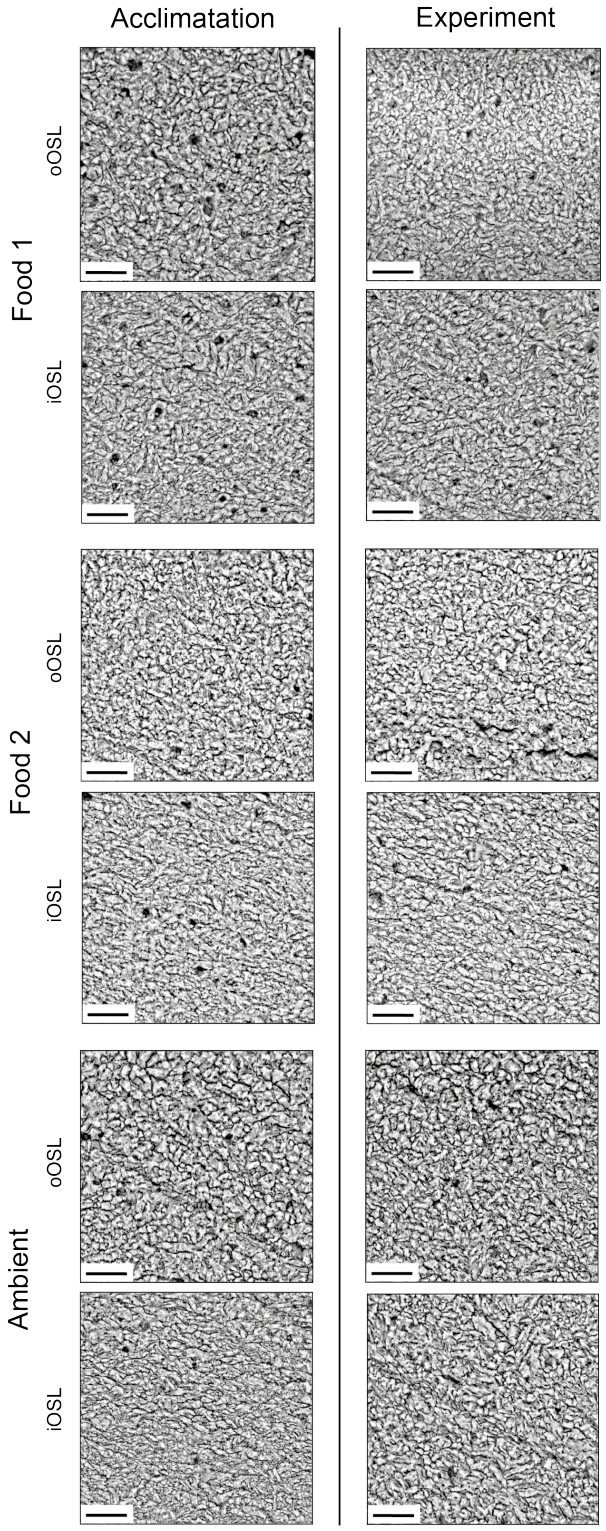
Acclimatation
Experiment
Food 1
Food 2
Ambient
oOSL
iOSL
oOSL
iOSL
oOSL
iOSL

830

Fig. 8. SEM images of *Arctica islandica* shell microstructures formed during the acclimation phase at AWI (left column) and during the food experiment (right column). Scale bars = 4 µm.

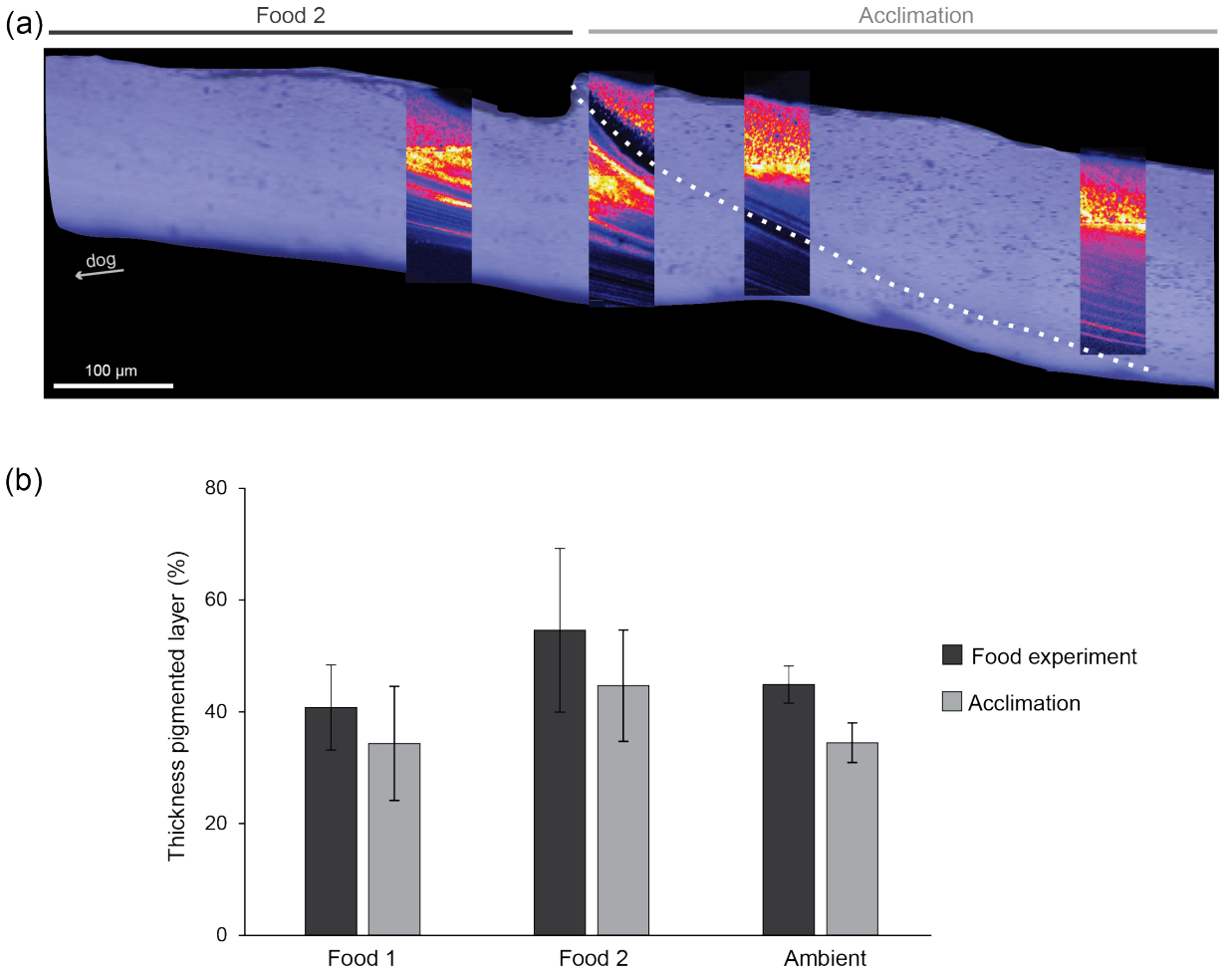

Fig. 9. Effects of diet on shell pigment distribution. (a) Raman spectral maps of the 1524 cm^{-1} band representing the distribution of the polyenes in the shell cultured with food type 2. Dotted line marks the start of the experiment. dog = direction of growth. (b) The graph shows the thickness of the pigmented layer over the whole shell thickness before and during the food experiments.

840 **Table 1.** List of the studied specimens of *Arctica islandica* and experimental conditions.

Sample ID	Locality	Age	Experiment	Treatment
A2	Maine	5	Temperature	10 °C + 15 °C
A4	Maine	4	Temperature	10 °C + 15 °C
A5	Maine	4	Temperature	10 °C + 15 °C
S12	Kiel Bay	1	Diet	Food 1
S14	Kiel Bay	1	Diet	Food 1
S15	Kiel Bay	1	Diet	Food 1
G11	Kiel Bay	1	Diet	Food 2
G12	Kiel Bay	1	Diet	Food 2
G15	Kiel Bay	1	Diet	Food 2
N13	Kiel Bay	1	Diet	No additional food
N15	Kiel Bay	1	Diet	No additional food

841

842 **Table 2.** Details of the pigment composition of the *Arctica islandica* shells used in the food experiment.
843 The position of the major polyene peaks R_1 and R_4 in the Raman spectrum is indicated together with the
844 number of single and double carbon bonds of the pigment molecular chain (N_1 and N_4). Each shell was
845 analyzed in the portions formed before and during the experimental phase.

Sample ID	Shell portion	R_1 (cm^{-1})	R_4 (cm^{-1})	N_1	N_4
S12	Acclimation	1130.9	1515.2	9.7	10.8
	Food 1	1121.4	1515.3	12.1	10.7
S14	Acclimation	1133.2	1519.4	9.3	10.2
	Food 1	1132.2	1518.6	9.5	10.3
S15	Acclimation	1129.5	1516.5	10.0	10.6
	Food 1	1132.1	1519.8	9.5	10.1
G11	Acclimation	1132.6	1518.4	9.4	10.3
	Food 2	1129.5	1517.0	10.0	10.5
G12	Acclimation	1131.7	1518.7	9.6	10.3
	Food 2	1132.1	1518.2	9.5	10.4
G15	Acclimation	1132.4	1519.5	9.4	10.2
	Food 2	1128.0	1520.9	10.3	10.0
N13	Acclimation	1130.2	1515.6	9.9	10.7
	Ambient food	1131.4	1514.1	9.6	10.9
N15	Acclimation	1117.9	1516.0	13.3	10.6
	Ambient food	1130.7	1517.0	9.8	10.5
Average		1129.7 ± 4.2	1517.5 ± 2.0	10.1 ± 1.1	10.4 ± 0.3